Acta Cryst E CRYSTALLOGRAPHIC COMMUNICATIONS

ISSN 2056-9890

Crystal structure, Hirshfeld surface analysis, interaction energy and DFT studies of 4-[(4-allyl-2-methoxyphenoxy)methyl]-1-(4-methoxyphenyl)-1*H*-1,2,3-triazole

Abdelmaoujoud Taia,[a]* Mohamed Essaber,[a] Abdeljalil Aatif,[a] Karim Chkirate,[b] Tuncer Hökelek,[c] Joel T. Mague[d] and Nada Kheira Sebbar[b,e]

[a]Laboratory of Molecular Chemistry, Department of Chemistry, Faculty of Sciences Semlalia, University of Cadi Ayyad, BP 2390, 40001 Marrakech, Morocco, [b]Laboratoire de Chimie Organique Heterocyclique URAC 21, Pôle de Competence Pharmacochimie, Av. Ibn Battouta, BP 1014, Faculté des Sciences, Université Mohammed V, Rabat, Morocco, [c]Department of Physics, Hacettepe University, 06800 Beytepe, Ankara, Turkey, [d]Department of Chemistry, Tulane University, New Orleans, LA 70118, USA, and [e]Laboratoire de Chimie Appliquée et Environnement, Equipe de Chimie Bioorganique Appliquée, Faculté des Sciences, Université Ibn Zohr, Agadir, Morocco. *Correspondence e-mail: AbdelmaoujoudTaia2018@gmail.com

Received 6 May 2020
Accepted 22 May 2020

Edited by M. Weil, Vienna University of Technology, Austria

Keywords: crystal structure; triazole; hydrogen bonding; C—H···π(ring) interaction; π-stacking.

CCDC reference: 2005277

Supporting information: this article has supporting information at journals.iucr.org/e

In the title molecule, $C_{20}H_{21}N_3O_3$, the allyl substituent is rotated out of the plane of its attached phenyl ring [torsion angle 100.66 (15)°]. In the crystal, C—H_{Mthphn}···O_{Mthphn} (Mthphn = methoxyphenyl) hydrogen bonds lead to the formation of (100) layers that are connected into a three-dimensional network by C—H···π(ring) interactions, together with π–π stacking interactions [centroid-to-centroid distance = 3.7318 (10) Å] between parallel phenyl rings. Hirshfeld surface analysis indicates that the most important contributions to the crystal packing are from H···H (48.7%) and H···C/C···H (23.3%) interactions. Computational chemistry reveals that the C—H_{Mthphn}···O_{Mthphn} hydrogen bond energy is 47.1 kJ mol^{-1}. The theoretical structure, optimized by density functional theory (DFT) at the B3LYP/ 6–311 G(d,p) level, is compared with the experimentally determined molecular structure. The HOMO–LUMO behaviour was elucidated to determine the energy gap.

1. Chemical context

Clove essential oil is extracted from cloves, which come from a tree belonging to the Myrtaceae family (Chang & Miau, 1984), originating from the Moluccas in Indonesia. Eugenol ($C_{10}H_{12}O_2$) is the major constituent of clove essential oil with a percentage of 75–90% (Patra & Saxena, 2010). Eugenol is a molecule that belongs to the family of phenylpropenes; its aromatic ring, an alcohol function and an allylic entity explain its high reactivity. Several studies have revealed various biological activities for eugenol, including antiviral (Benencia & Courreges, 2000), anti-leishmania (Ueda-Nakamura *et al.*, 2006), antibacterial (Pathirana *et al.*, 2019), antifungal (Wang *et al.*, 2010), anti-inflammatory (Daniel *et al.*, 2009), anti-oxidant (Mahboub & Memmou., 2015), anesthetic analgesic (Guenette *et al.*, 2007), anticancer (Hussain *et al.*, 2011) or anti-diabetes (Mnafgui *et al.*, 2013) properties. On the other hand, 1,2,3-triazoles are known by their diverse biological activities being used as antileishmania (Teixeira *et al.*, 2018), antimicrobial (Glowacka *et al.*, 2019) or antiviral (Bankowska, *et al.*, 2014) agents. In this context, we have synthesized the title compound, (I), through cycloaddition reaction of 1-azido-4-methoxybenzene with 4-allyl-2-methoxy-1-(prop-2-ynyloxy)

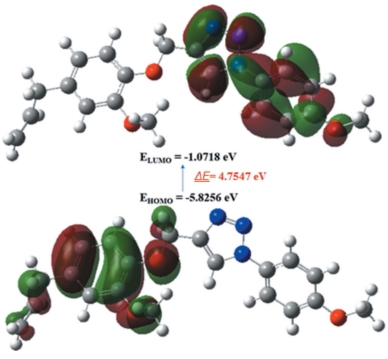

Table 1
Hydrogen-bond geometry (Å, °).

*Cg*3 is the centroid of the benzene ring *C* (C13–C18).

D—H···*A*	*D*—H	H···*A*	*D*···*A*	*D*—H···*A*
C6—H6···*Cg*3^{xiii}	0.964 (15)	2.825 (15)	3.5168 (15)	129.4 (11)
C19—H19*B*···O3^{xiv}	0.977 (18)	2.578 (18)	3.4587 (16)	150.0 (14)

Symmetry codes: (xiii) $x, -y-\frac{3}{2}, z-\frac{3}{2}$; (xiv) $-x+1, y+\frac{1}{2}, -z+\frac{3}{2}$.

benzene; the latter was previously prepared by O-alkylation of eugenol by propargile (Taia *et al.*, 2020).

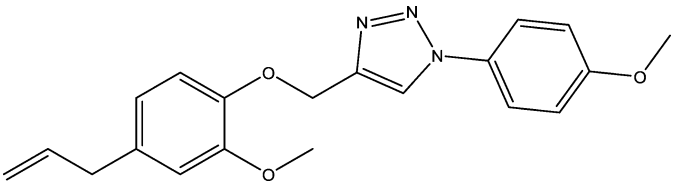

We report herein the synthesis, molecular and crystal structures of (I), along with the results of a Hirshfeld surface analysis, an interaction energy calculation, and a density functional theory (DFT) study.

2. Structural commentary

The title molecule is non-planar (Fig. 1), with the *A* (C1–C6) and *C* (C13–C18) benzene rings inclined to the *B* (C11/C12/N1–N3) triazole ring by 25.76 (4) and 24.97 (4)°, respectively. The allyl group is rotated out of the plane of the *A* ring as indicated by the C3—C4—C7—C8 torsion angle of 100.66 (15)°. Both methoxy groups are virtually coplanar with their attached rings with C3—C2—O2—C20 and C17—C16—O3—C19 torsion angles, respectively, of 5.04 (16) and 3.73 (16)°. There are no unusual bond lengths or bond angles in the molecule.

3. Supramolecular features

In the crystal structure, (100) layers are formed by C—H_{Mthphn}···O_{Mthphn} (Mthphn = methoxyphenyl) hydrogen bonds (Table 1, Fig. 2). These are stacked along the *a* axis

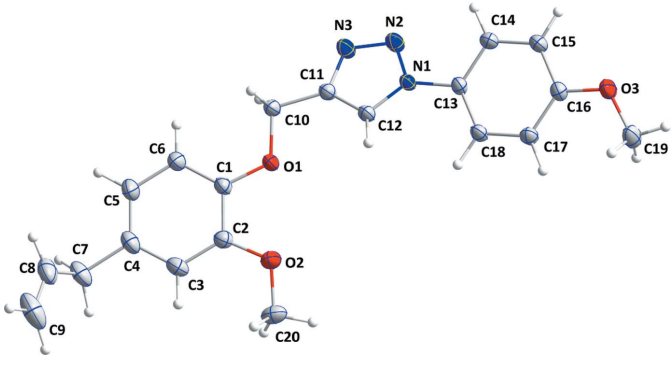

Figure 1
The molecular structure of (I) with the atom-numbering scheme. Displacement ellipsoids are drawn at the 50% probability level.

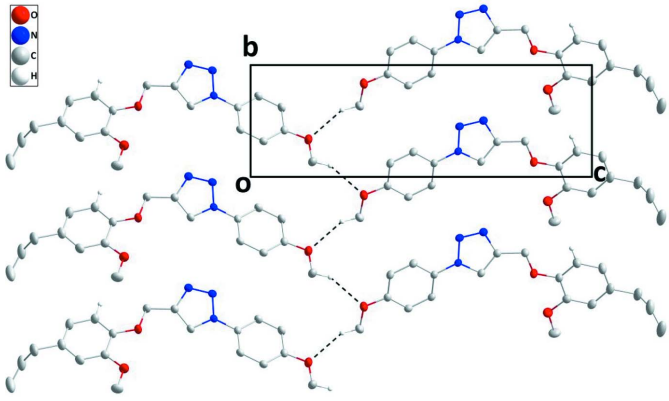

Figure 2
A portion of one layer viewed along the *a* axis, with C—H_{Mthphn}···O_{Mthphn} (Mthphn = methoxyphenyl) hydrogen bonds depicted by dashed lines.

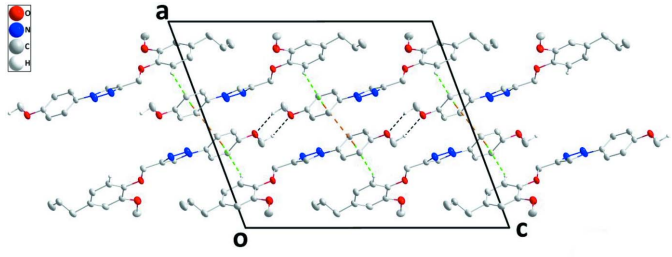

Figure 3
Projection of the crystal structure along the *b* axis. C—H_{Mthphn}···O_{Mthphn} (Mthphn = methoxyphenyl) hydrogen bonds and π–π stacking and C—H···π(ring) interactions are depicted, respectively, by black, orange and green dashed lines.

through C6—H6···*Cg*3($x, -\frac{1}{2}-y, -\frac{1}{2}+z$) interactions (Table 1) as well as through π—-π stacking interactions between inversion-related *C* rings [*Cg*3···*Cg*3($1-x, -y, 1-z$] with a centroid-to-centroid distance of 3.7318 (10) Å (Fig. 3).

4. Hirshfeld surface analysis

In order to visualize and quantify the intermolecular interactions in the crystal of (I), a Hirshfeld surface (HS) analysis (Hirshfeld, 1977; Spackman & Jayatilaka, 2009) was carried out by using *Crystal Explorer 17.5* (Turner *et al.*, 2017). In the HS plotted over d_{norm} (Fig. 4), the white surface indicates contacts with distances equal to the sum of van der Waals radii, and the red and blue colours indicate distances shorter or longer than the van der Waals radii, respectively (Venkatesan *et al.*, 2016). The bright-red spots appearing near hydrogen atoms (H6 and H19*B*), and near O3 indicate their roles in hydrogen bonding; they also appear as blue and red regions corresponding to positive (hydrogen-bond donors) and negative (hydrogen-bond acceptors) potentials on the HS mapped over electrostatic potential (Spackman *et al.*, 2008; Jayatilaka *et al.*, 2005), as shown in Fig. 5. The HS plotted over the shape-index (Fig. 6) clearly reveals π–π stacking inter-

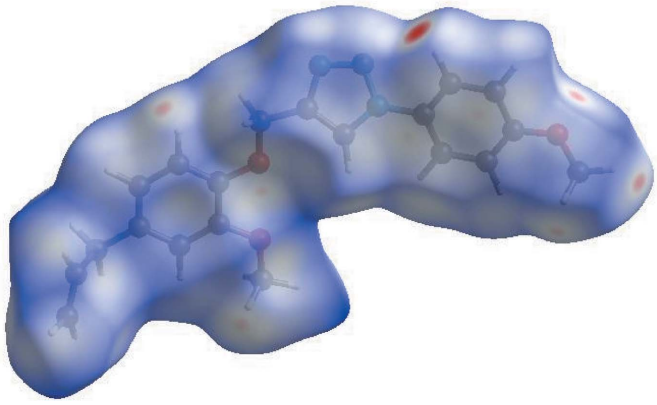

Figure 4
View of the three-dimensional Hirshfeld surface of the title compound plotted over d_{norm} in the range of −0.2587 to 1.3813 a.u..

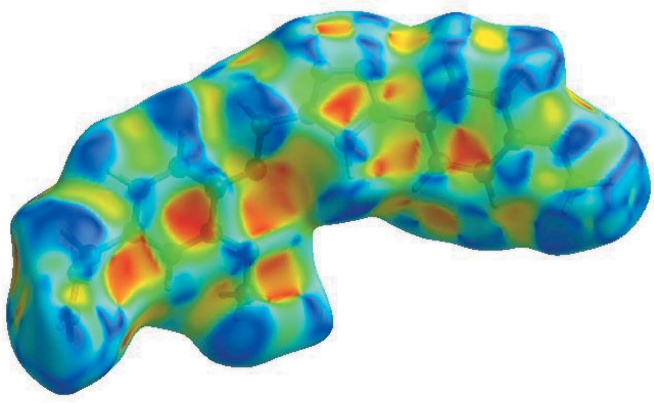

Figure 6
Hirshfeld surface of the title compound plotted over shape-index.

actions (visualized as red and blue areas) in (I), as discussed above.

The overall two-dimensional fingerprint plot, Fig. 7*a*, and those delineated into H···H, H···C/C···H, H···N/N···H, H···O/O···H, C···C, N···C/C···N, O···C/C···O and O···N/N···O contacts (McKinnon *et al.*, 2007) are illustrated in Fig. 7*b–i*, respectively, together with their relative contributions to the Hirshfeld surface. The most important interaction is H···H contributing 48.7% to the overall crystal packing, which is reflected in Fig. 7*b* as widely scattered points of high density due to the large hydrogen content of the molecule with the tip at $d_e = d_i = 0.95$ Å. In the presence of C—H···π interactions, the pair of characteristic wings of H···C/C···H contacts (23.3% contribution to the HS, Fig. 7*c*) has the tips at $d_e + d_i = 2.68$ Å. The pair of scattered points of spikes in the fingerprint plot delineated into H···N/N···H contacts (12.3% contribution, Fig. 7*d*) has a distribution of points with small and slightly larger tips at $d_e + d_i = 2.72$ and 2.70 Å, respectively. The H···O/O···H contacts (Fig. 7*e*, 11.3% contribution) have a symmetric distribution of points with the tips at $d_e + d_i = 2.48$ Å. The C···C contacts, Fig. 7*f*, have an arrow-shaped distribution of points with the tip at $d_e = d_i = 1.68$ Å. Finally, N···C/C···N (Fig. 7*g*), O···C/C···O (Fig. 7*h*) and O···N/N···O (Fig. 7*i*) interactions contribute only 1.0%, 0.9% and 0.6%, respectively, to the overall HS and thus have minor significance.

The Hirshfeld surface analysis confirms the importance of H-atom contacts in establishing the packing. The large number of H···H and H···C/C···H interactions suggest that van der Waals interactions and hydrogen bonding play the major roles in the crystal packing (Hathwar *et al.*, 2015).

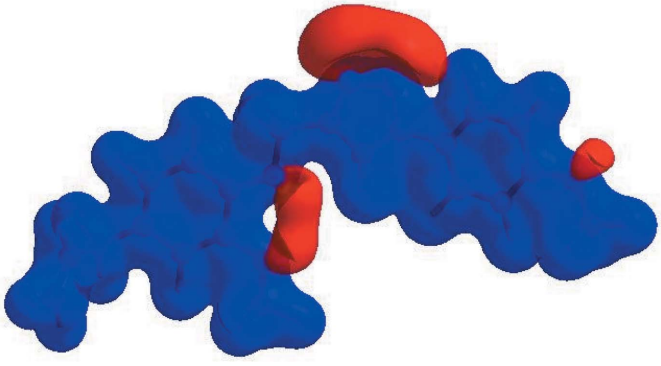

Figure 5
View of the three-dimensional Hirshfeld surface of the title compound plotted over electrostatic potential energy in the range −0.0500 to 0.0500 a.u..

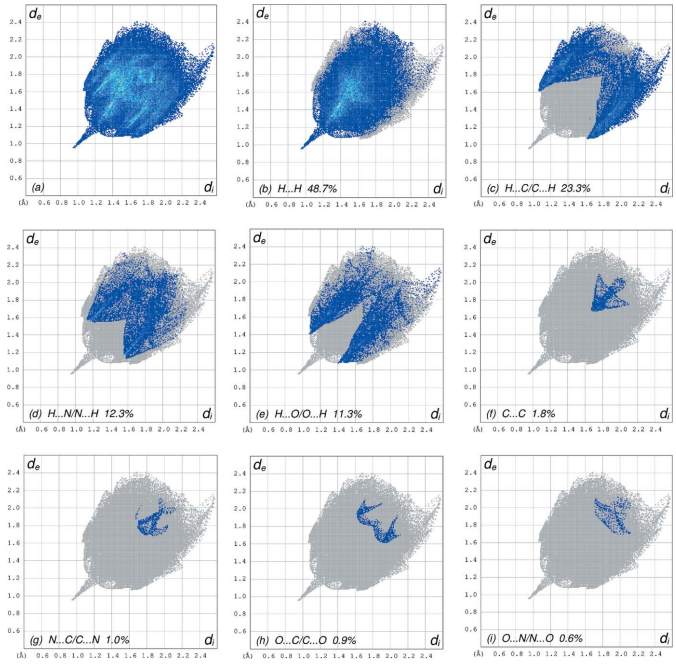

Figure 7
Two-dimensional fingerprint plots for (I), showing (*a*) all interactions, and delineated into (*b*) H···H, (*c*) H···C/C···H, (*d*) H···N/N···H, (*e*) H···O/O···H, (*f*) C···C, (*g*) N···C/C···N, (*h*) O···C/C···O and (i) O···N/N···O interactions. d_i and d_e refer to the closest internal and external distances (in Å) from given points on the Hirshfeld surface contacts.

Table 2
Comparison of selected bond length and angles (Å, °) between exerimental data (X-ray) and theory [B3LYP/6–311G(d,p)].

Bonds/angles	X-ray	B3LYP/6–311G(d,p)
O1—C1	1.3712 (12)	1.39510
O1—C10	1.4279 (12)	1.45830
O2—C2	1.3673 (13)	1.39818
O2—C20	1.4220 (14)	1.46747
O3—C16	1.3631 (12)	1.38746
O3—C19	1.4213 (15)	1.45298
N1—N2	1.3504 (13)	1.39727
N1—C12	1.3541 (13)	1.36977
N1—C13	1.4315 (13)	1.42427
N2—N3	1.3142 (13)	1.32619
N3—C11	1.3600 (13)	1.38002
C8—C9	1.312 (2)	1.33811
C1—O1—C10	117.19 (8)	117.72628
C2—O2—C20	117.19 (10)	117.20245
C16—O3—C19	117.42 (9)	118.93805
N2—N1—C12	110.77 (8)	110.09008
N2—N1—C13	119.89 (8)	120.52180
C12—N1—C13	129.33 (9)	129.38444
N3—N2—N1	107.21 (8)	106.61104
N2—N3—C11	108.86 (9)	109.15766
O1—C1—C6	125.33 (9)	124.33053

5. Interaction energy calculations

The intermolecular interaction energies were calculated using a CE–B3LYP/6–31G(d,p) energy model available in *Crystal Explorer 17.5* (Turner *et al.*, 2017), where a cluster of molecules was generated within a radius of 3.8 Å by default (Turner *et al.*, 2014). The total intermolecular energy (E_{tot}) is the sum of electrostatic (E_{ele}), polarization (E_{pol}), dispersion (E_{dis}) and exchange-repulsion (E_{rep}) energies (Turner *et al.*, 2015) with scale factors of 1.057, 0.740, 0.871 and 0.618, respectively (Mackenzie *et al.*, 2017). In (I), the relevant C19—H19*B*···O3 hydrogen-bonding interaction energies (in kJ mol^{-1}) were calculated as −20.6 (E_{ele}), −5.7 (E_{pol}), −49.3 (E_{dis}), 35.4 (E_{rep}) and −47.1 (E_{tot}).

6. DFT calculations

Density functional theory (DFT) using standard B3LYP functional and 6–311 G(d,p) basis-set calculations (Becke, 1993) as implemented in *GAUSSIAN 09* (Frisch *et al.*, 2009) was used to optimize the molecular structure of (I) in the gas phase. Theoretical and experimental results in terms of bond lengths and angles are in good agreement (Table 2).

The highest-occupied molecular orbital (HOMO) and the lowest-unoccupied molecular orbital (LUMO) together with the energy gap between them ($\Delta E = E_{LUMO} - E_{HOMO}$) are shown in Fig. 8. Table 3 collates calculated energies, including those for E_{HOMO} and E_{LUMO}, electronegativity (χ), hardness (η), potential (μ), electrophilicity (ω) and softness (σ).

7. Database survey

An eugenol 4-allyl-2-methoxyphenol analogue has been reported by Ghosh *et al.* (2005). Others similar compounds have also been reported (Ogata *et al.*, 2000; Yoo *et al.*, 2005; Sadeghian *et al.*, 2008; Ma *et al.* 2010).

Table 3
Calculated energies and other parameters for (I).

Total Energy *TE* (eV)	−31679.5273
E_{HOMO} (eV)	−5.8256
E_{LUMO} (eV)	−1.0718
Gap, ΔE (eV)	4.7547
Dipole moment, μ (Debye)	2.6382
Ionization potential, I (eV)	5.8256
Electron affinity, A	1.0718
Electronegativity, χ	3.4491
Hardness, η	2.3773
Electrophilicity index, ω	2.5021
Softness, σ	0.4206
Fraction of electron transferred, ΔN	0.7468

8. Synthesis and crystallization

To a solution of 4-allyl-2-methoxy-1-(prop-2-ynyloxy) benzene (0.4 ml, 2.5 mmol) in anhydrous acetonitrile, 1-azido-4-methoxybenzene (0.30 ml, 2.5 mmol) and 10 mg copper (I) iodide (CuI) were added. The mixture was refluxed for 2 h. After cooling, the reaction mixture was extracted three times with dichloromethane. The organic phase was dried with sodium sulfate and purified by column chromatography on silica gel, eluent hexane–ethyl acetate (v/v = 80/20). Colourless crystals were isolated when the solvent was allowed to evaporate (yield: 88%).

9. Refinement

Crystal data, data collection and structure refinement details are summarized in Table 4. Hydrogen atoms were located in a difference-Fourier map and were refined freely.

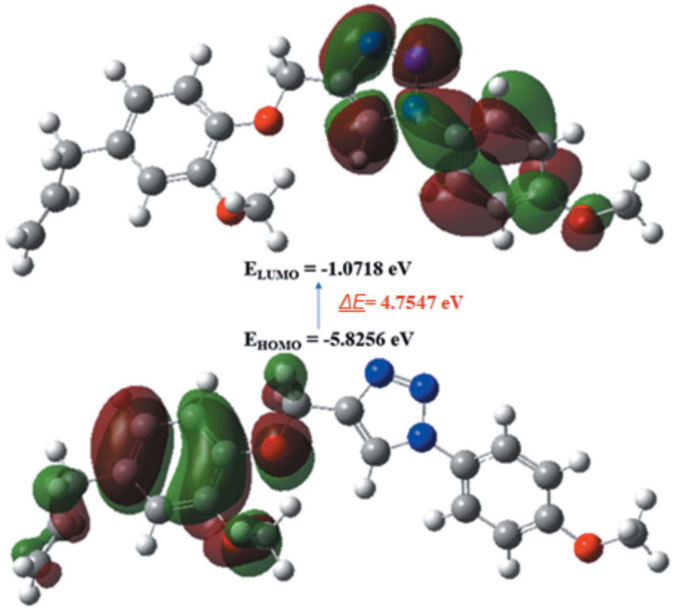

Figure 8
HOMO and LUMO of (I), and the energy band gap between them.

Table 4
Experimental details.

Crystal data	
Chemical formula	$C_{20}H_{21}N_3O_3$
M_r	351.40
Crystal system, space group	Monoclinic, $P2_1/c$
Temperature (K)	150
a, b, c (Å)	16.212 (3), 5.9584 (12), 19.450 (4)
β (°)	110.537 (3)
V (Å^3)	1759.5 (6)
Z	4
Radiation type	Mo $K\alpha$
μ (mm^{-1})	0.09
Crystal size (mm)	0.38 × 0.33 × 0.32
Data collection	
Diffractometer	Bruker *SMART APEX* CCD
Absorption correction	Multi-scan (*SADABS*; Krause *et al.*, 2015)
T_{min}, T_{max}	0.88, 0.97
No. of measured, independent and observed [$I > 2\sigma(I)$] reflections	32548, 4788, 3978
R_{int}	0.027
(sin $\theta/\lambda)_{max}$ (Å^{-1})	0.689
Refinement	
$R[F^2 > 2\sigma(F^2)]$, $wR(F^2)$, S	0.044, 0.132, 1.09
No. of reflections	4788
No. of parameters	319
H-atom treatment	All H-atom parameters refined
$\Delta\rho_{max}$, $\Delta\rho_{min}$ (e Å^{-3})	0.54, −0.22

Computer programs: *APEX3* and *SAINT* (Bruker, 2016), *SHELXT* (Sheldrick, 2015*a*), *SHELXL2018/1* (Sheldrick, 2015*b*), *DIAMOND* (Brandenburg & Putz, 2012) and *publCIF* (Westrip, 2010).

Funding information

JTM thanks Tulane University for support of the Tulane Crystallography Laboratory. TH is grateful to Hacettepe University Scientific Research Project Unit (grant No. 013 D04 602 004).

References

Bankowska, E., Balzarini, J., Głowacka, I. E. & Wróblewski, A. E. (2014). *Monatsh. Chem.* **145**, 663–673.
Becke, A. D. (1993). *J. Chem. Phys.* **98**, 5648–5652.
Benencia, F. & Courreges, M. C. (2000). *Phytother. Res.* **14**, 495–500.
Brandenburg, K. & Putz, H. (2012). *DIAMOND*, Crystal Impact GbR, Bonn, Germany.
Bruker (2016). *APEX3* and *SAINT*. Bruker AXS Inc., Madison, Wisconsin, USA.
Chang, H. T. & Miau, R. H. (1984). *Fl. Reipubl. Popularis Sin.* **53**, 28–135.
Daniel, A. N., Sartoretto, S. M., Schmidt, G., Caparroz-Assef, S. M., Bersani-Amado, C. A. & Cuman, R. K. N. (2009). *Rev. Bras. Farmacogn.* **19**, 212–217.
Frisch, M. J., Trucks, G. W., Schlegel, H. B., Scuseria, G. E., Robb, M. A., Cheeseman, J. R., *et al.* (2009). *GAUSSIAN09*. Gaussian Inc., Wallingford, CT, US
Ghosh, R., Nadiminty, N., Fitzpatrick, J. E., Alworth, W. L., Slaga, T. J. & Kumar, A. P. (2005). *J. Biol. Chem.* **280**, 5812–5819.
Glowacka, I. E., Grzonkowski, P., Lisiecki, P. & Kalinowski, L. (2019). *Arch. Pharm.* **352**, 1–4.
Guenette, S. A., Helie, P., Beaudry, F. & Vachon, P. (2007). *J. Vet. Anesth. Analg.*. **34**, 164–170.
Hathwar, V. R., Sist, M., Jørgensen, M. R. V., Mamakhel, A. H., Wang, X., Hoffmann, C. M., Sugimoto, K., Overgaard, J. & Iversen, B. B. (2015). *IUCrJ*, **2**, 563–574.
Hirshfeld, H. L. (1977). *Theor. Chim. Acta*, **44**, 129–138.
Hussain, A., Brahmbhatt, K., Priyani, A., Ahmed, M., Rizvi, T. A. & Sharma, C. (2011). *Cancer Biother. Radiopharm.* **26**, 519–527.
Jayatilaka, D., Grimwood, D. J., Lee, A., Lemay, A., Russel, A. J., Taylor, C., Wolff, S. K., Cassam-Chenai, P. & Whitton, A. (2005). *TONTO - A System for Computational Chemistry. Available at: http://hirshfeldsurface.net/*
Krause, L., Herbst-Irmer, R., Sheldrick, G. M. & Stalke, D. (2015). *J. Appl. Cryst.* **48**, 3–10.
Ma, Y.-T., Li, H.-Q., Shi, X.-W., Zhang, A.-L. & Gao, J.-M. (2010). *Acta Cryst.* E**66**, o2946.
Mackenzie, C. F., Spackman, P. R., Jayatilaka, D. & Spackman, M. A. (2017). *IUCrJ*, **4**, 575–587.
Mahboub, R. & Memmou, F. (2015). *Nat. Prod. Res.* **29**, 966–971.
McKinnon, J. J., Jayatilaka, D. & Spackman, M. A. (2007). *Chem. Commun.* pp. 3814–3816.
Mnafgui, K., Kaanich, F., Derbali, A., Hamden, K., Derbali, F., Slama, S., Allouche, N. & Elfeki, A. (2013). *Arch. Physiol. & Biochem.* **119**, 225–233.
Ogata, M., Hoshi, M., Urano, S. & Endo, T. (2000). *Chem. Pharm. Bull.* **48**, 1467–1469.
Pathirana, H. N. K. S., Wimalasena, S. H. M. P., De Silva, B. C. J., Hossain, S., **Gang-Joon** & **Heo** (2019). *Vet. Res.* **56**, 31–38.
Patra, A. K. & Saxena, J. (2010). *Phytochemistry*, **71**, 1198–1222.
Sadeghian, H., Seyedi, S. M., Saberi, M. R., Arghiani, Z. & Riazi, M. (2008). *Bioorg. Med. Chem.* **16**, 890–901.
Sheldrick, G. M. (2015*a*). *Acta Cryst.* A**71**, 3–8.
Sheldrick, G. M. (2015*b*). *Acta Cryst.* C**71**, 3–8.
Spackman, M. A. & Jayatilaka, D. (2009). *CrystEngComm*, **11**, 19–32.
Spackman, M. A., McKinnon, J. J. & Jayatilaka, D. (2008). *CrystEngComm*, **10**, 377–388.
Taia, A., Essaber, M., Hökelek, T., Aatif, A., Mague, J. T., Alsalme, A. & Al-Zaqri, N. (2020). *Acta Cryst.* E**76**, 344–348.
Teixeira, R. R., Gazolla, P. A. R., da Silva, A. M., Borsodi, M. P. G., Bergmann, B. R., Ferreira, R. S., Vaz, B. G., Vasconcelos, G. A. & Lima, W. P. (2018). *Eur. J. Med. Chem.* **146**, 274–286.
Turner, M. J., Grabowsky, S., Jayatilaka, D. & Spackman, M. A. (2014). *J. Phys. Chem. Lett.* **5**, 4249–4255.
Turner, M. J., McKinnon, J. J., Wolff, S. K., Grimwood, D. J., Spackman, P. R., Jayatilaka, D. & Spackman, M. A. (2017). *CrystalExplorer17*. The University of Western Australia.
Turner, M. J., Thomas, S. P., Shi, M. W., Jayatilaka, D. & Spackman, M. A. (2015). *Chem. Commun.* **51**, 3735–3738.
Ueda-Nakamura, T., Mendonça-Filho, R. R., Morgado-Díaz, J. A., Korehisa Maza, P., Prado Dias Filho, B., Aparício Garcia Cortez, D., Alviano, D. S., Rosa, M. S., Lopes, A. H., Alviano, C. S. & Nakamura, C. V. (2006). *Parasitol. Int.* **55**, 99–105.
Venkatesan, P., Thamotharan, S., Ilangovan, A., Liang, H. & Sundius, T. (2016). *Spectrochim. Acta Part A*, **153**, 625–636.
Wang, C., Zhang, J., Chen, H., Fan, Y. & Shi, Z. (2010). *Trop. Plant. Pathol.* **35**, 137–143.
Westrip, S. P. (2010). *J. Appl. Cryst.* **43**, 920–925.
Yoo, C. B., Han, K. T., Cho, K. S., Ha, J., Park, H. J., Nam, J. H., Kil, U. H. & Lee, K. T. (2005). *Cancer Lett.* **225**, 41–52.

supporting information

Acta Cryst. (2020). E**76**, 962-966 [https://doi.org/10.1107/S2056989020006994]

Crystal structure, Hirshfeld surface analysis, interaction energy and DFT studies of 4-[(4-allyl-2-methoxyphenoxy)methyl]-1-(4-methoxyphenyl)-1*H*-1,2,3-triazole

Abdelmaoujoud Taia, Mohamed Essaber, Abdeljalil Aatif, Karim Chkirate, Tuncer Hökelek, Joel T. Mague and Nada Kheira Sebbar

Computing details

Data collection: *APEX3* (Bruker, 2016); cell refinement: *SAINT* (Bruker, 2016); data reduction: *SAINT* (Bruker, 2016); program(s) used to solve structure: *SHELXT* (Sheldrick, 2015*a*); program(s) used to refine structure: *SHELXL2018/1* (Sheldrick, 2015*b*); molecular graphics: *DIAMOND* (Brandenburg & Putz, 2012); software used to prepare material for publication: *publCIF* (Westrip, 2010).

4-[(4-Allyl-2-methoxyphenoxy)methyl]-1-(4-methoxyphenyl)-1*H*-1,2,3-triazole

Crystal data

$C_{20}H_{21}N_3O_3$
M_r = 351.40
Monoclinic, $P2_1/c$
a = 16.212 (3) Å
b = 5.9584 (12) Å
c = 19.450 (4) Å
β = 110.537 (3)°
V = 1759.5 (6) Å^3
Z = 4
$F(000)$ = 744
D_x = 1.327 Mg m^{-3}
Mo $K\alpha$ radiation, λ = 0.71073 Å
Cell parameters from 9905 reflections
θ = 2.2–29.3°
μ = 0.09 mm^{-1}
T = 150 K
Block, colourless
0.38 × 0.33 × 0.32 mm

Data collection

Bruker SMART APEX CCD diffractometer
Radiation source: fine-focus sealed tube
Graphite monochromator
Detector resolution: 8.3333 pixels mm^{-1}
φ and ω scans
Absorption correction: multi-scan (*SADABS*; Krause *et al.*, 2015)
T_{min} = 0.88, T_{max} = 0.97
32548 measured reflections
4788 independent reflections
3978 reflections with $I > 2\sigma(I)$
R_{int} = 0.027
θ_{max} = 29.3°, θ_{min} = 2.2°
h = −22→21
k = −8→8
l = −26→26

Refinement

Refinement on F^2
Least-squares matrix: full
$R[F^2 > 2\sigma(F^2)]$ = 0.044
$wR(F^2)$ = 0.132
S = 1.09
4788 reflections
319 parameters
0 restraints
Primary atom site location: dual

Secondary atom site location: difference Fourier map	$w = 1/[\sigma^2(F_o^2) + (0.0858P)^2 + 0.1761P]$ where $P = (F_o^2 + 2F_c^2)/3$
Hydrogen site location: difference Fourier map	$(\Delta/\sigma)_{max} < 0.001$
All H-atom parameters refined	$\Delta\rho_{max} = 0.54$ e Å^{-3}
	$\Delta\rho_{min} = -0.22$ e Å^{-3}

Special details

Experimental. The diffraction data were obtained from 3 sets of 400 frames, each of width 0.5° in ω, colllected at φ = 0.00, 90.00 and 180.00° and 2 sets of 800 frames, each of width 0.45° in φ, collected at ω = –30.00 and 210.00°. The scan time was 10 sec/frame.

Geometry. All esds (except the esd in the dihedral angle between two l.s. planes) are estimated using the full covariance matrix. The cell esds are taken into account individually in the estimation of esds in distances, angles and torsion angles; correlations between esds in cell parameters are only used when they are defined by crystal symmetry. An approximate (isotropic) treatment of cell esds is used for estimating esds involving l.s. planes.

Refinement. Refinement of F^2 against ALL reflections. The weighted R-factor wR and goodness of fit S are based on F^2, conventional R-factors R are based on F, with F set to zero for negative F^2. The threshold expression of $F^2 > 2$sigma(F^2) is used only for calculating R-factors(gt) etc. and is not relevant to the choice of reflections for refinement. R-factors based on F^2 are statistically about twice as large as those based on F, and R- factors based on ALL data will be even larger.

Fractional atomic coordinates and isotropic or equivalent isotropic displacement parameters (Å²)

	x	*y*	*z*	U_{iso}*/U_{eq}
O1	0.22952 (5)	−0.13314 (13)	0.17036 (4)	0.02658 (18)
O2	0.13208 (6)	0.21761 (14)	0.12923 (5)	0.0343 (2)
O3	0.45455 (5)	0.16414 (14)	0.66870 (4)	0.03039 (19)
N1	0.35850 (6)	−0.22912 (14)	0.39234 (4)	0.02175 (18)
N2	0.36971 (7)	−0.45263 (15)	0.38817 (5)	0.0295 (2)
N3	0.34449 (6)	−0.50475 (15)	0.31817 (5)	0.0293 (2)
C1	0.19702 (6)	−0.09553 (18)	0.09610 (5)	0.0237 (2)
C2	0.14239 (7)	0.09424 (18)	0.07352 (6)	0.0253 (2)
C3	0.10348 (7)	0.14141 (19)	−0.00049 (6)	0.0298 (2)
H3	0.0643 (10)	0.270 (3)	−0.0155 (8)	0.039 (4)*
C4	0.11724 (7)	0.0034 (2)	−0.05366 (6)	0.0314 (2)
C5	0.17275 (8)	−0.1789 (2)	−0.03076 (6)	0.0331 (3)
H5	0.1821 (11)	−0.278 (3)	−0.0671 (9)	0.043 (4)*
C6	0.21292 (7)	−0.2286 (2)	0.04393 (6)	0.0290 (2)
H6	0.2500 (9)	−0.359 (2)	0.0595 (8)	0.031 (3)*
C7	0.07032 (8)	0.0524 (3)	−0.13467 (7)	0.0394 (3)
H7A	0.0142 (12)	0.144 (3)	−0.1426 (10)	0.051 (5)*
H7B	0.0508 (15)	−0.099 (4)	−0.1622 (13)	0.086 (7)*
C8	0.12580 (9)	0.1689 (3)	−0.17069 (7)	0.0451 (3)
H8	0.1781 (14)	0.088 (3)	−0.1728 (11)	0.066 (5)*
C9	0.10758 (12)	0.3641 (4)	−0.20373 (8)	0.0597 (5)
H9	0.0469 (18)	0.449 (4)	−0.2068 (14)	0.099 (8)*
H9B	0.1442 (14)	0.434 (4)	−0.2293 (12)	0.071 (6)*
C10	0.28746 (7)	−0.31981 (18)	0.19593 (6)	0.0249 (2)
H10A	0.2564 (9)	−0.465 (2)	0.1772 (8)	0.028 (3)*
H10B	0.3377 (9)	−0.304 (2)	0.1801 (7)	0.026 (3)*
C11	0.31793 (6)	−0.31470 (17)	0.27769 (6)	0.0230 (2)
C12	0.32669 (7)	−0.13692 (17)	0.32445 (6)	0.0232 (2)

H12	0.3179 (9)	0.025 (2)	0.3173 (8)	0.031 (3)*
C13	0.38036 (6)	−0.12328 (16)	0.46256 (5)	0.0210 (2)
C14	0.44278 (7)	−0.22392 (18)	0.52340 (6)	0.0246 (2)
H14	0.4712 (9)	−0.363 (2)	0.5174 (8)	0.029 (3)*
C15	0.46548 (7)	−0.12254 (18)	0.59111 (6)	0.0249 (2)
H15	0.5101 (11)	−0.194 (3)	0.6325 (9)	0.040 (4)*
C16	0.42651 (6)	0.08019 (17)	0.59909 (5)	0.0226 (2)
C17	0.36412 (7)	0.17993 (17)	0.53822 (6)	0.0240 (2)
H17	0.3362 (10)	0.328 (3)	0.5429 (8)	0.039 (4)*
C18	0.34120 (7)	0.07693 (17)	0.46974 (5)	0.0232 (2)
H18	0.2975 (8)	0.148 (2)	0.4265 (7)	0.025 (3)*
C19	0.41329 (10)	0.3629 (2)	0.68101 (7)	0.0373 (3)
H19A	0.3554 (13)	0.341 (3)	0.6731 (10)	0.050 (5)*
H19B	0.4447 (11)	0.399 (3)	0.7326 (10)	0.047 (4)*
H19C	0.4223 (12)	0.480 (3)	0.6507 (10)	0.056 (5)*
C20	0.07124 (9)	0.3989 (2)	0.10918 (8)	0.0374 (3)
H20A	0.0124 (13)	0.347 (3)	0.0825 (11)	0.060 (5)*
H20B	0.0740 (10)	0.471 (3)	0.1585 (10)	0.047 (4)*
H20C	0.0901 (10)	0.514 (3)	0.0820 (9)	0.046 (4)*

Atomic displacement parameters (Å²)

	U^{11}	U^{22}	U^{33}	U^{12}	U^{13}	U^{23}
O1	0.0318 (4)	0.0271 (4)	0.0177 (4)	0.0090 (3)	0.0046 (3)	0.0019 (3)
O2	0.0408 (5)	0.0298 (4)	0.0294 (4)	0.0122 (3)	0.0088 (3)	0.0000 (3)
O3	0.0365 (4)	0.0303 (4)	0.0194 (4)	0.0041 (3)	0.0036 (3)	−0.0023 (3)
N1	0.0260 (4)	0.0191 (4)	0.0178 (4)	0.0022 (3)	0.0048 (3)	0.0024 (3)
N2	0.0424 (5)	0.0192 (4)	0.0227 (4)	0.0025 (4)	0.0063 (4)	0.0018 (3)
N3	0.0394 (5)	0.0216 (4)	0.0222 (4)	0.0017 (4)	0.0051 (4)	0.0006 (3)
C1	0.0232 (4)	0.0261 (5)	0.0187 (5)	0.0007 (4)	0.0035 (3)	0.0012 (4)
C2	0.0241 (5)	0.0244 (5)	0.0251 (5)	0.0012 (4)	0.0057 (4)	0.0009 (4)
C3	0.0269 (5)	0.0297 (5)	0.0272 (5)	0.0027 (4)	0.0025 (4)	0.0060 (4)
C4	0.0275 (5)	0.0396 (6)	0.0217 (5)	−0.0023 (4)	0.0018 (4)	0.0041 (4)
C5	0.0338 (6)	0.0409 (6)	0.0209 (5)	0.0036 (5)	0.0051 (4)	−0.0023 (5)
C6	0.0289 (5)	0.0317 (5)	0.0229 (5)	0.0057 (4)	0.0045 (4)	−0.0008 (4)
C7	0.0349 (6)	0.0502 (8)	0.0241 (6)	−0.0033 (5)	−0.0010 (4)	0.0065 (5)
C8	0.0337 (6)	0.0741 (10)	0.0234 (6)	0.0000 (6)	0.0047 (5)	0.0015 (6)
C9	0.0578 (9)	0.0807 (12)	0.0296 (7)	−0.0256 (9)	0.0014 (6)	0.0125 (7)
C10	0.0273 (5)	0.0240 (5)	0.0199 (5)	0.0057 (4)	0.0040 (4)	0.0003 (4)
C11	0.0238 (4)	0.0222 (5)	0.0207 (5)	0.0020 (3)	0.0051 (4)	0.0015 (4)
C12	0.0267 (5)	0.0221 (5)	0.0189 (5)	0.0035 (4)	0.0055 (4)	0.0036 (4)
C13	0.0240 (4)	0.0206 (4)	0.0170 (4)	−0.0005 (3)	0.0055 (3)	0.0017 (3)
C14	0.0270 (5)	0.0238 (5)	0.0217 (5)	0.0059 (4)	0.0070 (4)	0.0035 (4)
C15	0.0258 (5)	0.0264 (5)	0.0196 (5)	0.0043 (4)	0.0044 (4)	0.0042 (4)
C16	0.0247 (4)	0.0234 (5)	0.0185 (4)	−0.0017 (3)	0.0061 (3)	0.0005 (4)
C17	0.0287 (5)	0.0194 (4)	0.0225 (5)	0.0020 (4)	0.0074 (4)	0.0016 (4)
C18	0.0263 (5)	0.0206 (4)	0.0197 (5)	0.0024 (3)	0.0045 (4)	0.0042 (4)
C19	0.0553 (8)	0.0269 (6)	0.0247 (6)	0.0042 (5)	0.0079 (5)	−0.0040 (4)

C20	0.0363 (6)	0.0290 (6)	0.0471 (7)	0.0098 (5)	0.0148 (5)	0.0040 (5)

Geometric parameters (Å, º)

O1—C1	1.3712 (12)	C8—H8	0.99 (2)
O1—C10	1.4279 (12)	C9—H9	1.09 (3)
O2—C2	1.3673 (13)	C9—H9B	0.99 (2)
O2—C20	1.4220 (14)	C10—C11	1.4908 (14)
O3—C16	1.3631 (12)	C10—H10A	1.002 (14)
O3—C19	1.4213 (15)	C10—H10B	0.971 (14)
N1—N2	1.3504 (13)	C11—C12	1.3708 (15)
N1—C12	1.3541 (13)	C12—H12	0.978 (15)
N1—C13	1.4315 (13)	C13—C18	1.3812 (14)
N2—N3	1.3142 (13)	C13—C14	1.3942 (14)
N3—C11	1.3600 (13)	C14—C15	1.3764 (15)
C1—C6	1.3814 (15)	C14—H14	0.975 (14)
C1—C2	1.4082 (14)	C15—C16	1.3969 (15)
C2—C3	1.3827 (15)	C15—H15	0.970 (17)
C3—C4	1.3991 (17)	C16—C17	1.3921 (14)
C3—H3	0.974 (16)	C17—C18	1.3935 (14)
C4—C5	1.3808 (17)	C17—H17	1.010 (16)
C4—C7	1.5185 (16)	C18—H18	0.984 (13)
C5—C6	1.3995 (16)	C19—H19A	0.905 (19)
C5—H5	0.972 (17)	C19—H19B	0.977 (18)
C6—H6	0.964 (15)	C19—H19C	0.956 (19)
C7—C8	1.491 (2)	C20—H20A	0.96 (2)
C7—H7A	1.025 (18)	C20—H20B	1.037 (18)
C7—H7B	1.04 (2)	C20—H20C	0.979 (17)
C8—C9	1.312 (2)		

O1···O2	2.5723 (13)	C18···H12	2.871 (15)
O1···H12	2.870 (14)	C19···H17	2.543 (15)
O2···H10A^{i}	2.681 (14)	C19···O1^{vi}	3.3285 (19)
O3···H19B^{ii}	2.579 (18)	C20···H3	2.508 (15)
N2···C18^{iii}	3.3320 (15)	C20···H10A^{i}	2.938 (15)
N2···H14	2.532 (15)	H3···H7A	2.43 (2)
N2···H18^{iii}	2.864 (13)	H3···H20A	2.38 (3)
N2···H14^{iv}	2.812 (15)	H3···H20C	2.31 (2)
N3···H12^{iii}	2.834 (12)	H5···H7B	2.52 (3)
N3···H15^{iv}	2.848 (18)	H6···H10A	2.34 (2)
C12···C15^{v}	3.5436 (18)	H6···H10B	2.30 (2)
C13···C15^{v}	3.3633 (17)	H6···C17^{ix}	2.791 (14)
C13···C14^{v}	3.4679 (17)	H6···C18^{ix}	2.955 (15)
C14···C14^{v}	3.5463 (18)	H7A···H9	2.37 (3)
C14···C18^{v}	3.5668 (18)	H7B···H9^{x}	2.50 (4)
C19···C1^{vi}	3.589 (2)	H8···N3^{ix}	2.808 (1)
C19···C10^{vi}	3.4746 (19)	H9···H20B^{xi}	2.50 (3)
C1···H20C^{iii}	2.856 (18)	H9B···O2^{xii}	2.837 (5)

C3···H20C	2.792 (17)	H10B···C16^{ix}	2.976 (14)
C3···H20A	2.82 (2)	H10B···C19^{xii}	2.897 (13)
C4···H20A^{vii}	2.88 (2)	H12···H18	2.377 (19)
C5···H20A^{vii}	2.98 (2)	H14···H14^{iv}	2.107 (19)
C6···H20C^{iii}	2.811 (17)	H15···H19C^{iii}	2.51 (3)
C6···H10A	2.814 (4)	H15···H19B^{ii}	2.53 (2)
C6···H10B	2.748 (13)	H17···H19A	2.44 (2)
C9···H7B^{viii}	2.96 (2)	H17···H19C	2.26 (2)
C10···H6	2.517 (15)	H18···C8^{vi}	2.970 (13)
C12···H18	2.776 (13)	H19A···O1^{vi}	2.67 (2)
C15···H19C^{iii}	2.830 (18)	H19A···C1^{vi}	2.91 (2)
C17···H19C	2.725 (18)	H19C···H10B^{vi}	2.55 (2)
C17···H19A	2.843 (19)		

C1—O1—C10	117.19 (8)	C11—C10—H10A	110.0 (8)
C2—O2—C20	117.19 (10)	O1—C10—H10B	109.5 (8)
C16—O3—C19	117.42 (9)	C11—C10—H10B	109.6 (8)
N2—N1—C12	110.77 (8)	H10A—C10—H10B	109.9 (11)
N2—N1—C13	119.89 (8)	N3—C11—C12	108.73 (9)
C12—N1—C13	129.33 (9)	N3—C11—C10	121.31 (9)
N3—N2—N1	107.21 (8)	C12—C11—C10	129.94 (9)
N2—N3—C11	108.86 (9)	N1—C12—C11	104.42 (9)
O1—C1—C6	125.33 (9)	N1—C12—H12	121.7 (8)
O1—C1—C2	115.27 (9)	C11—C12—H12	133.8 (8)
C6—C1—C2	119.40 (10)	C18—C13—C14	120.55 (9)
O2—C2—C3	125.30 (10)	C18—C13—N1	120.54 (8)
O2—C2—C1	115.02 (9)	C14—C13—N1	118.91 (9)
C3—C2—C1	119.68 (10)	C15—C14—C13	119.62 (10)
C2—C3—C4	121.15 (10)	C15—C14—H14	120.6 (8)
C2—C3—H3	118.9 (9)	C13—C14—H14	119.7 (8)
C4—C3—H3	119.9 (9)	C14—C15—C16	120.42 (9)
C5—C4—C3	118.60 (10)	C14—C15—H15	118.3 (9)
C5—C4—C7	121.24 (11)	C16—C15—H15	121.3 (9)
C3—C4—C7	120.15 (11)	O3—C16—C17	125.29 (9)
C4—C5—C6	120.98 (11)	O3—C16—C15	114.93 (9)
C4—C5—H5	119.5 (10)	C17—C16—C15	119.78 (9)
C6—C5—H5	119.5 (10)	C16—C17—C18	119.70 (9)
C1—C6—C5	120.15 (10)	C16—C17—H17	120.7 (9)
C1—C6—H6	119.3 (9)	C18—C17—H17	119.6 (9)
C5—C6—H6	120.5 (9)	C13—C18—C17	119.94 (9)
C8—C7—C4	114.32 (10)	C13—C18—H18	120.2 (8)
C8—C7—H7A	109.4 (10)	C17—C18—H18	119.8 (8)
C4—C7—H7A	110.7 (10)	O3—C19—H19A	111.9 (11)
C8—C7—H7B	106.6 (13)	O3—C19—H19B	104.5 (10)
C4—C7—H7B	108.6 (13)	H19A—C19—H19B	110.0 (15)
H7A—C7—H7B	106.9 (16)	O3—C19—H19C	108.7 (11)
C9—C8—C7	125.01 (16)	H19A—C19—H19C	111.8 (15)
C9—C8—H8	117.5 (12)	H19B—C19—H19C	109.6 (15)

C7—C8—H8	117.4 (12)	O2—C20—H20A	111.5 (11)
C8—C9—H9	118.7 (14)	O2—C20—H20B	105.0 (9)
C8—C9—H9B	123.1 (13)	H20A—C20—H20B	110.1 (14)
H9—C9—H9B	118.0 (18)	O2—C20—H20C	111.3 (9)
O1—C10—C11	106.67 (8)	H20A—C20—H20C	111.8 (15)
O1—C10—H10A	111.1 (8)	H20B—C20—H20C	106.8 (14)

C12—N1—N2—N3	−0.64 (12)	N2—N3—C11—C12	−0.22 (12)
C13—N1—N2—N3	179.75 (8)	N2—N3—C11—C10	178.55 (9)
N1—N2—N3—C11	0.52 (12)	O1—C10—C11—N3	154.23 (9)
C10—O1—C1—C6	2.77 (15)	O1—C10—C11—C12	−27.29 (15)
C10—O1—C1—C2	−178.10 (9)	N2—N1—C12—C11	0.49 (11)
C20—O2—C2—C3	5.04 (16)	C13—N1—C12—C11	−179.94 (9)
C20—O2—C2—C1	−174.39 (10)	N3—C11—C12—N1	−0.16 (11)
O1—C1—C2—O2	2.06 (14)	C10—C11—C12—N1	−178.80 (10)
C6—C1—C2—O2	−178.75 (10)	N2—N1—C13—C18	−155.77 (10)
O1—C1—C2—C3	−177.40 (9)	C12—N1—C13—C18	24.69 (15)
C6—C1—C2—C3	1.79 (16)	N2—N1—C13—C14	25.16 (14)
O2—C2—C3—C4	−179.27 (10)	C12—N1—C13—C14	−154.37 (10)
C1—C2—C3—C4	0.13 (16)	C18—C13—C14—C15	−0.03 (15)
C2—C3—C4—C5	−1.79 (17)	N1—C13—C14—C15	179.04 (9)
C2—C3—C4—C7	177.07 (10)	C13—C14—C15—C16	−0.10 (16)
C3—C4—C5—C6	1.55 (18)	C19—O3—C16—C17	3.73 (16)
C7—C4—C5—C6	−177.30 (11)	C19—O3—C16—C15	−176.25 (10)
O1—C1—C6—C5	177.07 (10)	C14—C15—C16—O3	−179.83 (9)
C2—C1—C6—C5	−2.03 (17)	C14—C15—C16—C17	0.19 (15)
C4—C5—C6—C1	0.35 (18)	O3—C16—C17—C18	179.87 (9)
C5—C4—C7—C8	−80.52 (17)	C15—C16—C17—C18	−0.16 (15)
C3—C4—C7—C8	100.66 (15)	C14—C13—C18—C17	0.06 (15)
C4—C7—C8—C9	−121.28 (16)	N1—C13—C18—C17	−178.99 (9)
C1—O1—C10—C11	176.23 (8)	C16—C17—C18—C13	0.03 (15)

Symmetry codes: (i) *x*, *y*+1, *z*; (ii) −*x*+1, *y*−1/2, −*z*+3/2; (iii) *x*, *y*−1, *z*; (iv) −*x*+1, −*y*−1, −*z*+1; (v) −*x*+1, −*y*, −*z*+1; (vi) *x*, −*y*+1/2, *z*+1/2; (vii) −*x*, −*y*, −*z*; (viii) −*x*, *y*+1/2, −*z*−1/2; (ix) *x*, −*y*−1/2, *z*−1/2; (x) −*x*, *y*−1/2, −*z*−1/2; (xi) −*x*, −*y*+1, −*z*; (xii) *x*, −*y*+1/2, *z*−1/2.

Hydrogen-bond geometry (Å, º)

*Cg*3 is the centroid of the benzene ring *C* (C13–C18).

D—H···*A*	*D*—H	H···*A*	*D*···*A*	*D*—H···*A*
C6—H6···*Cg*3^{xiii}	0.964 (15)	2.825 (15)	3.5168 (15)	129.4 (11)
C19—H19*B*···O3^{xiv}	0.977 (18)	2.578 (18)	3.4587 (16)	150.0 (14)

Symmetry codes: (xiii) *x*, −*y*−3/2, *z*−3/2; (xiv) −*x*+1, *y*+1/2, −*z*+3/2.